

Charm production from proton-proton collisions

Wei Liu, Che Ming Ko, and Su Houn Lee*

¹*Cyclotron Institute and Physics Department, Texas A&M University, College Station, Texas 77843-3366, USA*

We evaluate the cross sections for charmed hadron production from proton-proton reactions $pp \rightarrow \bar{D}^0 p \Lambda_c^+$ and $pp \rightarrow \bar{D}^{*0} p \Lambda_c^+$ using a hadronic Lagrangian. With empirical coupling constants and cutoff parameters in the form factors, sum of their cross sections at center-of-mass energy of 11.5 GeV is about 1 μ b and is comparable to measured inclusive cross section for charmed hadron production from proton-proton reactions. The cross section decreases to about 1 nb at 40 MeV above threshold.

PACS numbers: 25.75.-q, 13.75.Lb, 14.40.Gx, 14.40.Lb

I. INTRODUCTION

For reactions involving hadrons that consist of charm quarks, a hadronic model with interaction Lagrangian based on the SU(4) flavor symmetry was first introduced in Ref. [1]. With empirical coupling constants and introducing form factors at interaction vertices, this model gives a J/ψ absorption cross section by pion or rho meson [2–4] that is comparable to that needed in the comover model for understanding the observed suppression of J/ψ production in relativistic heavy ion collisions [5,6]. Extending the Lagrangian to include the interactions between charmed hadrons and baryons, the model has also been used to study J/ψ absorption by nucleons [7] and charm photoproduction on nucleons [8]. In both cases, the theoretical cross sections are comparable to those known empirically. The model has further been used to calculate the cross section for charm production from π -N interactions [9], which is relevant to charmed meson production in relativistic heavy ion collisions [10], and the cross sections for charmed meson scattering by hadrons [11,12]. In the present paper, the same hadronic Lagrangian is used to evaluate charmed hadron production from proton-proton collisions. Motivated by future experiments at proposed accelerator facility at the German Heavy Ion Research Center [13], there are already studies on these reactions based on the meson-exchange model [14,15]. However, effects due to off-shellness of exchanged mesons have been neglected in these studies. As in our previous studies of J/ψ absorption by nucleon [7] and photoproduction of J/ψ on nucleons [8], we do not make the on-shell approximation in evaluating the charmed meson production cross section from proton-proton collisions.

This paper is organized as follows. In Section II, we introduce the interaction Lagrangians that are needed to evaluate the cross sections for charm production from proton-proton collisions. The two reactions $pp \rightarrow \bar{D}^0 p \Lambda_c$ and $pp \rightarrow \bar{D}^{*0} p \Lambda_c$ are then discussed in Section III. We

show in this section the amplitudes for these reactions and calculate their cross sections due to contributions from pion, rho meson, D , and D^* exchanges. The total cross section for charm production in proton-proton collisions is given in Section IV and compared to available experimental data. Finally, a brief summary is given in Section V.

II. THE HADRONIC MODEL

Possible reactions for charmed hadron production in proton-proton collisions near threshold are $pp \rightarrow \bar{D}^0 p \Lambda_c^+$ and $pp \rightarrow \bar{D}^{*0} p \Lambda_c^+$. Cross sections for these reactions can be evaluated using the same Lagrangian introduced in Refs. [7,8,11,12] for studying charmed meson scattering by hadrons. This Lagrangian is based on the gauged SU(4) flavor symmetry but with empirical masses. The coupling constants are taken, if possible, from empirical information. Otherwise, the SU(4) relations are used to relate unknown coupling constants to known ones. Form factors are introduced at interaction vertices with empirically determined cutoff parameters.

A. interaction Lagrangians

From the formalism described in Refs. [7,8,11,12], the interaction Lagrangian densities that are relevant to present study are given as follows:

$$\begin{aligned}\mathcal{L}_{\pi NN} &= -ig_{\pi NN} \bar{N} \gamma_5 \vec{\tau} N \cdot \vec{\pi}, \\ \mathcal{L}_{\rho NN} &= g_{\rho NN} \bar{N} \left(\gamma^\mu \vec{\tau} \cdot \vec{\rho}_\mu + \frac{\kappa_\rho}{2m_N} \sigma_{\mu\nu} \vec{\tau} \cdot \partial_\mu \vec{\rho}_\nu \right) N, \\ \mathcal{L}_{\pi DD^*} &= ig_{\pi DD^*} D^{*\mu} \vec{\tau} \cdot (\bar{D} \partial_\mu \vec{\pi} - \partial_\mu \bar{D} \vec{\pi}) + \text{H.c.}, \\ \mathcal{L}_{\rho DD} &= ig_{\rho DD} (D \vec{\tau} \partial_\mu \bar{D} - \partial_\mu D \vec{\tau} \bar{D}) \cdot \vec{\rho}^\mu, \\ \mathcal{L}_{\rho D^* D^*} &= ig_{\rho D^* D^*} [(\partial_\mu D^{*\nu} \vec{\tau} \bar{D}_\nu^* - D^{*\nu} \vec{\tau} \partial_\mu \bar{D}_\nu^*) \cdot \vec{\rho}^\mu \\ &\quad + (D^{*\nu} \vec{\tau} \cdot \partial_\mu \vec{\rho}^\nu - \partial_\mu D^{*\nu} \vec{\tau} \cdot \vec{\rho}_\nu) \bar{D}^{*\mu}\end{aligned}$$

*Permanent address: Department of Physics and Institute of Physics and Applied Physics, Yonsei University, Seoul 120-749, Korea

$$\begin{aligned}
& + D^{*\mu}(\vec{\tau} \cdot \vec{\rho}^\nu \partial_\mu \bar{D}_\nu^* - \vec{\tau} \cdot \partial_\mu \vec{\rho}^\nu \bar{D}_\nu^*), \\
\mathcal{L}_{DN\Lambda_c} &= ig_{DN\Lambda_c}(\bar{N}\gamma_5\Lambda_c\bar{D} + D\bar{\Lambda}_c\gamma_5 N), \\
\mathcal{L}_{D^*N\Lambda_c} &= g_{D^*N\Lambda_c}(\bar{N}\gamma_\mu\Lambda_c D^{*\mu} + \bar{D}^{*\mu}\bar{\Lambda}_c\gamma_\mu N), \\
\mathcal{L}_{\pi\Lambda_c\Sigma_c} &= ig_{\pi\Lambda_c\Sigma_c}\bar{\Lambda}_c\gamma^5\vec{\Sigma}_c \cdot \vec{\pi} + \text{H.c.}, \\
\mathcal{L}_{\rho\Lambda_c\Sigma_c} &= g_{\rho\Lambda_c\Sigma_c}\bar{\Lambda}_c\gamma^\mu\vec{\Sigma}_c \cdot \vec{\rho}_\mu + \text{H.c.}, \\
\mathcal{L}_{DN\Sigma_c} &= ig_{DN\Sigma_c}(\bar{N}\gamma^5\vec{\tau} \cdot \vec{\Sigma}_c\bar{D} + D\vec{\tau} \cdot \vec{\Sigma}_c\gamma^5 N), \\
\mathcal{L}_{D^*N\Sigma_c} &= g_{D^*N\Sigma_c}(\bar{N}\gamma^\mu\vec{\tau} \cdot \vec{\Sigma}_c\bar{D}_\mu^* + D_\mu^*\vec{\tau} \cdot \vec{\Sigma}_c\gamma^\mu N). \quad (1)
\end{aligned}$$

In the above, $\vec{\tau}$ are Pauli spin matrices, and $\vec{\pi}$ and $\vec{\rho}$ denote, respectively, the pion and rho meson isospin triplet, while $D = (D^+, D^0)$ and $D^* = (D^{*+}, D^{*0})$ denote, respectively, the pseudoscalar and vector charmed meson doublets.

B. coupling constants

For coupling constants, we use the following empirical values: $g_{\pi NN} = 13.5$ [16], $g_{\rho NN} = 3.25$, and $\kappa_\rho = 6.1$ [17], and $g_{\pi DD^*} = 5.56$ [18], and $g_{\rho DD} = g_{\rho D^* D^*} = 2.52$ [12]. Other coupling constants, which are not known empirically, are obtained using SU(4) relations [3,7,8,12], i.e.,

$$\begin{aligned}
g_{D^*N\Lambda_c} &= -\sqrt{3}g_{\rho NN} = -5.6, \\
g_{DN\Lambda_c} &= \frac{3-2\alpha_D}{\sqrt{3}}g_{\pi NN} \simeq g_{\pi NN} = 13.5, \\
g_{\pi\Lambda_c\Sigma_c} &\simeq -\frac{2\alpha_D}{\sqrt{3}}g_{\pi NN}, \quad g_{DN\Sigma_c} \simeq (1-2\alpha_D)g_{DN\Lambda_c}, \\
g_{D^*N\Sigma_c} &= -g_{\rho NN}. \quad (2)
\end{aligned}$$

where $\alpha_D = D/(D+F) \simeq 0.64$ [19] with D and F being the coefficients for usual D -type and F -type couplings.

C. form factors

To take into account finite sizes of hadrons, form factors are introduced at interaction vertices. In previous studies on J/ψ absorption and charmed hadron scattering by hadrons, monopole form factors have been used. Following the work on J/ψ absorption by nucleons [7], the form factors at πNN and ρNN vertices are taken to have the form:

$$F_1(t) = \frac{\Lambda^2 - m^2}{\Lambda^2 - t}, \quad (3)$$

with t being the squared four momentum of exchanged pion or rho meson, while those at πDD^* , ρDD , $\rho D^* D^*$, $DN\Lambda_c$, $D^*N\Lambda_c$, $DN\Sigma_c$, and $D^*N\Sigma_c$ vertices, that involve heavy virtual charm mesons or baryons, are

$$F_2(\mathbf{q}^2) = \frac{\Lambda^2}{\Lambda^2 + \mathbf{q}^2}. \quad (4)$$

with \mathbf{q} being the three momentum transfer in the center-of-mass frame for t and u channels or momentum of initial or final particles in center-of-mass frame for s channel [12]. As in Refs. [16,17], we take $\Lambda_{\pi NN} = 1.3$ GeV and $\Lambda_{\rho NN} = 1.4$ GeV. For the cutoff parameters in $F_2(\mathbf{q}^2)$, they are taken to be 0.42 GeV. As discussed later in Section III, this cutoff parameter is needed in a similar hadronic model to reproduce the empirical cross section for $pp \rightarrow K^+ p \Lambda$ reaction at center-of-mass energy from threshold to a few GeV,

III. CHARMED HADRON PRODUCTION FROM PROTON-PROTON COLLISIONS

In proton-proton collisions at low energies, charm production is dominated by three particle final states. Two possible reactions are $pp \rightarrow \bar{D}^0 p \Lambda_c$ and $pp \rightarrow \bar{D}^{*0} p \Lambda_c$. In the following, we discuss their contributions separately.

A. $pp \rightarrow \bar{D}^0 p \Lambda_c^+$

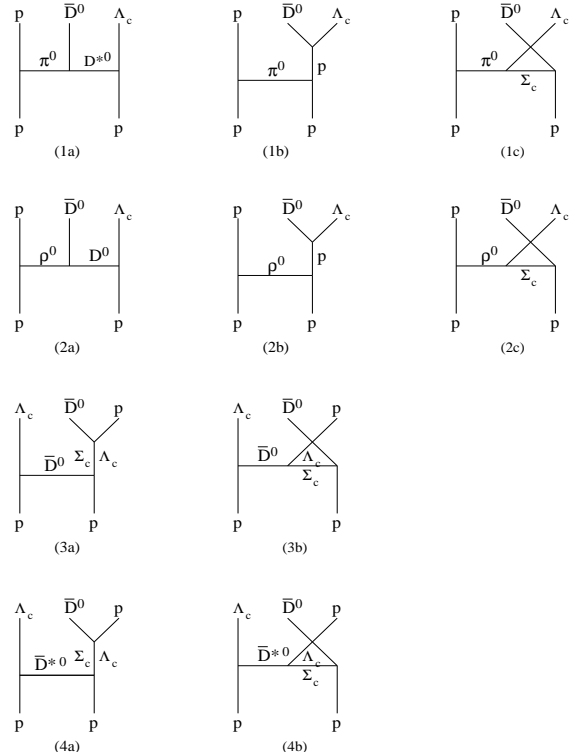


FIG. 1. Charmed hadron production from $pp \rightarrow \bar{D}^0 p \Lambda_c^+$.

Diagrams for the reaction $pp \rightarrow \bar{D}^0 p \Lambda_c^+$ are shown in Fig. 1. They involve the exchange of pion ((1a) – (1c)), rho meson ((2a) – (2c)), D ((3a) – (3b)), and D^* ((4a) – (4b)). Amplitudes for the four processes are given by

$$\begin{aligned}
\mathcal{M}_1 &= -ig_{\pi NN} \bar{p}(p_3) \gamma_5 p(p_1) \frac{1}{t - m_\pi^2} \\
&\quad \times (\mathcal{M}_{1a} + \mathcal{M}_{1b} + \mathcal{M}_{1c}), \\
\mathcal{M}_2 &= g_{\rho NN} \bar{p}(p_3) \left[\gamma^\mu + i \frac{\kappa_\rho}{2m_N} \sigma^{\alpha\mu} (p_1 - p_3)_\alpha \right] p(p_1) \\
&\quad \times \left[-g_{\mu\nu} + \frac{(p_1 - p_3)_\mu (p_1 - p_3)_\nu}{m_\rho^2} \right] \\
&\quad \times \frac{1}{t - m_\rho^2} (\mathcal{M}_{2a}^\nu + \mathcal{M}_{2b}^\nu + \mathcal{M}_{2c}^\nu), \\
\mathcal{M}_3 &= ig_{D N \Lambda_c} \bar{\Lambda}_c(p_3) \gamma_5 p(p_1) \frac{1}{t - m_D^2} \\
&\quad \times (\mathcal{M}_{3a} + \mathcal{M}_{3b}), \\
\mathcal{M}_4 &= g_{D^* N \Lambda_c} \bar{\Lambda}_c(p_3) \gamma^\mu p(p_1) \\
&\quad \times \left[-g_{\mu\nu} + \frac{(p_1 - p_3)_\mu (p_1 - p_3)_\nu}{m_{D^*}^2} \right] \\
&\quad \times \frac{1}{t - m_{D^*}^2} (\mathcal{M}_{4a}^\nu + \mathcal{M}_{4b}^\nu), \tag{5}
\end{aligned}$$

where p_1 and p_3 are, respectively, four momenta of initial and final baryons on the left side of a diagram, and $t = (p_1 - p_3)^2$ is the square of nucleon momentum transfer. The amplitudes M_{ia} , M_{ib} , and M_{ic} are for the subprocesses $\pi^0 p \rightarrow \bar{D}^0 \Lambda_c^+$, $\rho^0 p \rightarrow \bar{D}^0 \Lambda_c^+$, $\bar{D}^0 p \rightarrow \bar{D}^0 p^+$, and $\bar{D}^{*0} p \rightarrow \bar{D}^0 p$ involving exchanged virtual mesons, and they are given explicitly by

$$\begin{aligned}
\mathcal{M}_{1a} &= -g_{\pi DD^*} g_{D^* N \Lambda_c} \frac{1}{q^2 - m_{D^*}^2} (k_1 + k_3)_\mu \\
&\quad \times \left[g^{\mu\nu} - \frac{(k_1 - k_3)_\mu (k_1 - k_3)_\nu}{m_{D^*}^2} \right] \bar{\Lambda}_c \gamma_\nu p, \\
\mathcal{M}_{1b} &= g_{\pi NN} g_{D N \Lambda_c} \frac{1}{s_1 - m_N^2} \bar{\Lambda}_c (m_N - \not{k}_1 - \not{k}_2) p, \\
\mathcal{M}_{1c} &= g_{\pi \Lambda_c \Sigma_c} g_{D N \Sigma_c} \frac{1}{u - m_{\Sigma_c}^2} \bar{\Lambda}_c (\not{k}_2 - \not{k}_3 - m_{\Sigma_c}) p, \\
\mathcal{M}_{2a}^\mu &= ig_{D N \Lambda_c} g_{\rho DD} \frac{1}{q^2 - m_D^2} (2k_3 - k_1)^\mu \bar{\Lambda}_c \gamma^5 p, \\
\mathcal{M}_{2b}^\mu &= ig_{\rho NN} g_{D N \Lambda_c} \frac{1}{s_1 - m_N^2} \bar{\Lambda}_c \gamma^5 (\not{k}_1 + \not{k}_2 + m_N) \\
&\quad \times \left(\gamma^\mu + i \frac{\kappa_\rho}{2m_N} \sigma^{\beta\mu} k_{1\beta} \right) p, \\
\mathcal{M}_{2c}^\mu &= ig_{\rho \Lambda_c \Sigma_c} g_{D N \Sigma_c} \frac{1}{u - m_{\Sigma_c}^2} \\
&\quad \times \bar{\Lambda}_c \gamma^\mu (\not{k}_2 - \not{k}_3 + m_{\Sigma_c}) \gamma^5 p, \\
\mathcal{M}_{3a} &= g_{D N \Lambda_c}^2 \frac{1}{s_1 - m_{\Lambda_c}^2} \bar{p} (\not{k}_1 + \not{k}_2 - m_{\Lambda_c}) p, \\
\mathcal{M}_{3b} &= g_{D N \Lambda_c}^2 \frac{1}{u - m_{\Lambda_c}^2} \bar{p} (\not{k}_2 - \not{k}_3 - m_{\Lambda_c}) p,
\end{aligned}$$

$$\begin{aligned}
\mathcal{M}_{4a}^\mu &= ig_{D^* N \Lambda_c} g_{D N \Lambda_c} \frac{1}{s_1 - m_{\Lambda_c}^2} \\
&\quad \times \bar{p} \gamma^5 (\not{k}_1 + \not{k}_2 + m_{\Lambda_c}) \gamma^\mu p, \\
\mathcal{M}_{4b}^\mu &= ig_{D^* N \Lambda_c} g_{D N \Lambda_c} \frac{1}{u - m_{\Lambda_c}^2} \\
&\quad \times \bar{p} \gamma^\mu (\not{k}_2 - \not{k}_3 + m_{\Lambda_c}) \gamma^5 p. \tag{6}
\end{aligned}$$

Here, k_1 and k_3 are momenta of initial and final mesons, while k_2 and k_4 are momenta of initial and final baryons in the two-body subprocesses; and $q^2 = (k_1 - k_3)^2$ is the square of meson momentum transfer.

There is no interference between amplitudes involving exchange of pseudoscalar and vector mesons. Interferences between amplitudes involving exchange of pion and D meson as well as those between rho meson and D^* are unimportant due to the large mass difference between light and heavy mesons. Neglecting these interferences, the total cross section for the reaction $pp \rightarrow \bar{D}^0 p \Lambda_c^+$ is then given by the sum of the cross sections for the four processes in Fig. 1 and can be expressed in terms of off-shell cross sections for the subprocesses $\pi^0 p \rightarrow \bar{D}^0 \Lambda_c^+$, $\rho^0 p \rightarrow \bar{D}^0 \Lambda_c^+$, $\bar{D}^0 p \rightarrow \bar{D}^0 p$, and $\bar{D}^{*0} p \rightarrow \bar{D}^0 p$. Following the method of Ref. [8] for the reaction $J/\psi N \rightarrow D(D^*) \bar{D}(\bar{D}^*) N$, the spin-averaged differential cross section for the reaction $pp \rightarrow \bar{D}^0 p \Lambda_c^+$ can be written as

$$\begin{aligned}
&\frac{d\sigma_{pp \rightarrow \bar{D}^0 p \Lambda_c^+}}{dt ds_1} \\
&= \frac{g_{\pi NN}^2}{16\pi^2 s p_i^2} k \sqrt{s_1} (-t) \frac{1}{(t - m_\pi^2)^2} \sigma_{\pi^0 p \rightarrow \bar{D}^0 \Lambda_c^+}(s_1, t), \\
&\quad + \frac{3g_{\rho NN}^2}{32\pi^2 s p_i^2} k \sqrt{s_1} \frac{1}{(t - m_\rho^2)^2} [4(1 + \kappa_\rho)^2 \\
&\quad \times (-t - 2m_N^2) \kappa_\rho^2 \frac{(4m_N^2 - t)^2}{2m_N^2} + 4(1 + \kappa_\rho) \\
&\quad \times \kappa_\rho (4m_N^2 - t)] \sigma_{\rho^0 p \rightarrow \bar{D}^0 \Lambda_c^+}(s_1, t), \\
&\quad + \frac{g_{D N \Lambda_c}^2}{16\pi^2 s p_i^2} k \sqrt{s_1} [-t + (m_N - m_{\Lambda_c})^2] \frac{1}{(t - m_D^2)^2} \\
&\quad \times \sigma_{\bar{D}^0 p \rightarrow \bar{D}^0 p}(s_1, t) \\
&\quad + \frac{3g_{D^* N \Lambda_c}^2}{32\pi^2 s p_i^2} k \sqrt{s_1} \frac{1}{(t - m_{D^*}^2)^2} [-4t + 4(m_{\Lambda_c} - m_N)^2 \\
&\quad - 8m_{\Lambda_c} m_N + \frac{2(m_N^2 - m_{\Lambda_c}^2 - t)(m_N^2 - m_{\Lambda_c}^2 + t)}{m_{D^*}^2} \\
&\quad + \frac{2((m_{\Lambda_c} - m_N)^2 + t)t}{m_{D^*}^2}] \sigma_{D^{*0} p \rightarrow \bar{D}^0 p}(s_1, t). \tag{7}
\end{aligned}$$

In the above, p_i is the center-of-mass momentum of two initial protons, t is the squared four momentum transfer of exchanged meson, s is the squared center-of-mass energy, and s_1 and k are, respectively, the squared invariant mass and center-of-mass momentum of exchanged meson and the nucleon in the subprocesses. We have also included a factor of two to take into account contributions from interchanging two initial protons.

Since the charmed hadron production cross sections is sensitive to the value of cutoff parameters in the form factors at interaction vertices involving virtual charmed mesons and baryons, it is necessary to constrain this cutoff parameter empirically. Without exclusive cross sections available for charmed hadron production from proton-proton scattering, we resort to strange hadron production. Using the same hadronic model for kaon production from the reaction $pp \rightarrow K^+ p \Lambda$, this reaction can be described by similar diagrams in Fig.1 for the reaction $pp \rightarrow \bar{D}^0 p \Lambda_c^+$ with D^0 and Λ_c replaced by K^+ and Λ , respectively, in the final states. Also, the exchanged \bar{D}^0 in diagrams (3a) and (3b) as well as \bar{D}^{0*} in diagrams (4a) and (4b) are replaced by K and K^* , respectively, while intermediate off-shell charmed baryons are replaced by strange baryons. With empirical coupling constants $g_{\pi K K^*} = 3.25$ and $g_{\rho K K} = 3.25$, as well as others determined via SU(3) relations [20], the measured cross section can be reproduced with a cutoff parameter $\Lambda = 0.42$ GeV in the form factors $F_2(q^2)$ at vertices involving virtual strange mesons and baryons, as shown in Fig.2.

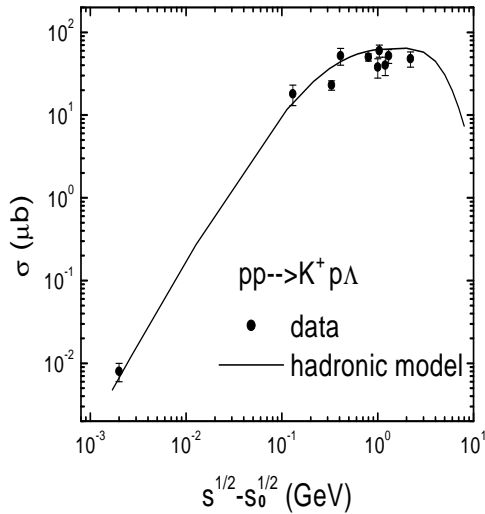


FIG. 2. Cross section for kaon production from the reaction $pp \rightarrow K^+ p \Lambda$ with cutoff parameter $\Lambda = 0.42$ GeV in the form factors at interaction vertices involving exchange of strange mesons. Filled circles are experimental data taken from Ref. [21]

Assuming that the same cutoff parameter $\Lambda = 0.42$ GeV is applicable at vertices involving virtual charmed mesons and baryons in charmed hadron production from proton-proton reactions, resulting cross sections for the reaction $pp \rightarrow \bar{D}^0 p \Lambda_c^+$ from the four possible processes of pion (solid curve), rho (dashed curve), D (dotted curve), and D^* (dash-dotted curve) exchanges as functions of center-of-mass energy are shown in Fig.3. It is seen that contributions from light meson exchange are more impor-

tant than those from heavy meson exchange. Although we consider diagrams (1a) and (2a) in Fig.1 as exchange of pion and rho meson, respectively, they actually involve exchange of heavy D^* and D mesons in the subprocess $\pi^0 p \rightarrow \bar{D}^0 \Lambda_c^+$ and $\rho^0 p \rightarrow \bar{D}^0 \Lambda_c^+$, respectively. Our results that main contributions to the reaction $pp \rightarrow p \bar{D}^0 \Lambda_c^+$ are due to exchange of light mesons are not inconsistent with conclusions in Ref. [14] that this reaction is dominated by heavy D meson exchange.

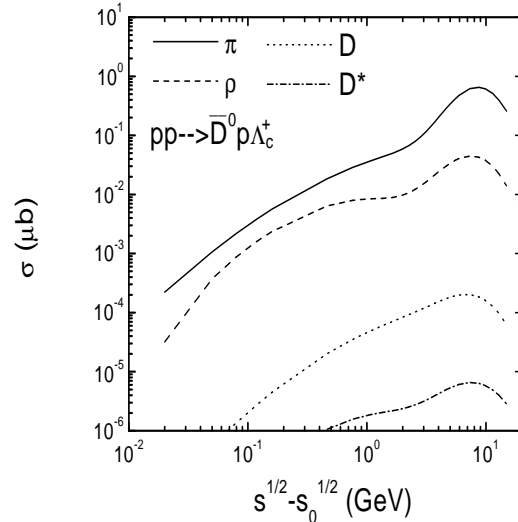


FIG. 3. Cross sections for charmed hadron production from the reaction $pp \rightarrow \bar{D}^0 p \Lambda_c^+$ due to pion (solid curve), rho meson (dashed curve), D (dotted curve), and D^* (dash-dotted curve).

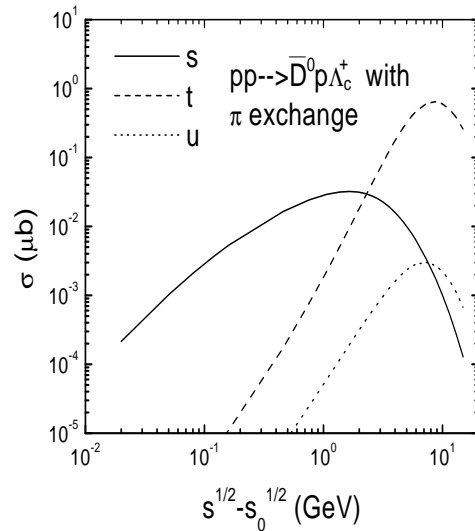


FIG. 4. Partial cross sections for $pp \rightarrow \bar{D}^0 p \Lambda_c^+$ due to contributions from different channels.

To see the relative contributions from s , t , and u channel diagrams in Fig.1, we show in Fig.4 the partial cross sections due to diagrams (1a), (1b), and (1c). It is seen that the t channel diagram (1a) dominates charmed hadron production cross section at high energies while the s channel diagram (1b) is most important near threshold. The contribution from the u channel diagram (1c) is much smaller than those from other two diagrams. Except near threshold, our results are thus similar to those found in Ref. [14], which uses the on-shell approximation for the subprocess $\pi p \rightarrow \bar{D}^0 \Lambda_c^+$ and does not include s and u channel diagrams.

B. $pp \rightarrow \bar{D}^{*0} p \Lambda_c^+$

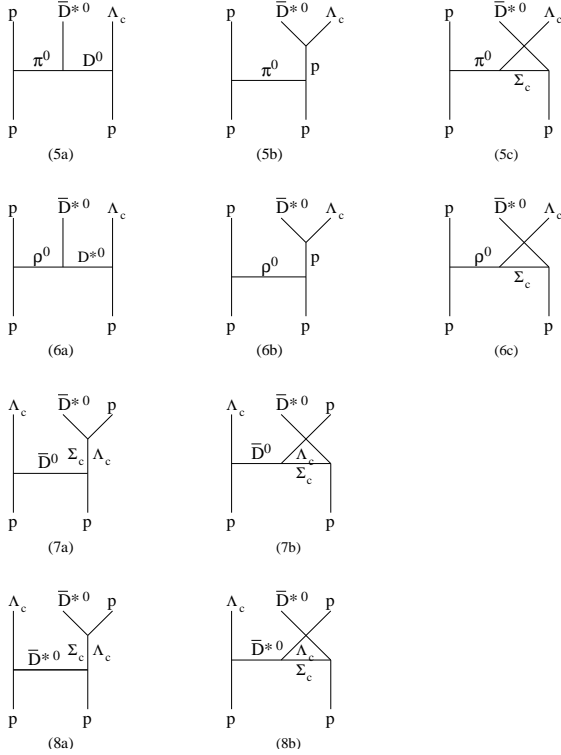


FIG. 5. Charmed hadron production from $pp \rightarrow \bar{D}^{*0} p \Lambda_c^+$.

For charm production from proton-proton collisions with $\bar{D}^{*0} p \Lambda_c^+$ in the final state, relevant diagrams are shown in Fig. 5. As for the reaction $pp \rightarrow \bar{D}^{*0} p \Lambda_c^+$, this reaction can proceed through pion, rho meson, D , and D^* exchanges. Amplitudes for the four processes can be evaluated with the interaction Lagrangians given in Section II, and they are given by

$$\mathcal{M}_5 = -ig_{\pi NN} \bar{p}(p_3) \gamma_5 p(p_1) \frac{1}{t - m_\pi^2} \times (\mathcal{M}_{5a}^\alpha + \mathcal{M}_{5b}^\alpha + \mathcal{M}_{5c}^\alpha) \epsilon_\alpha$$

$$\begin{aligned} \mathcal{M}_6 &= g_{\rho NN} \bar{p}(p_3) \left[\gamma^\mu + i \frac{\kappa_\rho}{2m_N} \sigma^{\alpha\mu} (p_1 - p_3)_\alpha \right] p(p_1) \\ &\times \left[-g_{\mu\nu} + \frac{(p_1 - p_3)_\mu (p_1 - p_3)_\nu}{m_\rho^2} \right] \\ &\times \frac{1}{t - m_\rho^2} (\mathcal{M}_{6a}^{\nu\alpha} + \mathcal{M}_{6b}^{\nu\alpha} + \mathcal{M}_{6c}^{\nu\alpha}) \epsilon_\alpha, \\ \mathcal{M}_7 &= ig_{DN\Lambda_c} \bar{\Lambda}_c(p_3) \gamma_5 p(p_1) \frac{1}{t - m_D^2} \\ &\times (\mathcal{M}_{7a}^\alpha + \mathcal{M}_{7b}^\alpha) \epsilon_\alpha, \\ \mathcal{M}_8 &= g_{D^* N \Lambda_c} \bar{\Lambda}_c(p_3) \gamma^\mu p(p_1) \\ &\times \left[-g_{\mu\nu} + \frac{(p_1 - p_3)_\mu (p_1 - p_3)_\nu}{m_{D^*}^2} \right] \\ &\times \frac{1}{t - m_{D^*}^2} (\mathcal{M}_{8a}^{\nu\alpha} + \mathcal{M}_{8b}^{\nu\alpha}) \epsilon_\alpha, \end{aligned} \quad (8)$$

where p_1 and p_3 are again, respectively, four momenta of initial and final baryons on the left side of a diagram and ϵ_α denotes the polarization vector of D^* meson in final state.

Expressions for individual amplitudes can be written as follows:

$$\begin{aligned} \mathcal{M}_{5a}^\mu &= -ig_{\pi DD^*} g_{DN\Lambda_c} \frac{1}{q^2 - m_D^2} (2k_1 - k_3)^\mu \bar{\Lambda}_c \gamma_5 p, \\ \mathcal{M}_{5b}^\mu &= -ig_{\pi NN} g_{D^* N \Lambda_c} \frac{1}{s_1 - m_N^2} \\ &\times \bar{\Lambda}_c \gamma^\mu (\not{k}_1 + \not{k}_2 + m_N) \gamma_5 p, \\ \mathcal{M}_{5c}^\mu &= ig_{\pi \Lambda_c \Sigma_c} g_{D^* N \Sigma_c} \frac{1}{u - m_{\Sigma_c}^2} \\ &\times \bar{\Lambda}_c \gamma_5 (\not{k}_2 - \not{k}_3 + m_{\Sigma_c}) \gamma^\mu p, \\ \mathcal{M}_{6a}^{\mu\nu} &= g_{D^* N \Lambda_c} g_{\rho D^* D^*} \frac{1}{q^2 - m_{D^*}^2} \\ &\times \left[g_{\alpha\beta} - \frac{(k_1 - k_3)_\alpha (k_1 - k_3)_\beta}{m_{D^*}^2} \right] \bar{\Lambda}_c \gamma^\alpha p \\ &\times [2k_1^\nu g^{\beta\mu} - (k_1 + k_3)^\beta g^{\mu\nu} + 2k_3^\mu g^{\beta\nu}], \\ \mathcal{M}_{6b}^{\mu\nu} &= g_{\rho NN} g_{D^* N \Lambda_c} \frac{1}{s_1 - m_N^2} \bar{\Lambda}_c \gamma^\nu (\not{k}_1 + \not{k}_2 + m_N) \\ &\times \left(\gamma^\mu + i \frac{\kappa_\rho}{2m_N} \sigma^{\beta\mu} k_{1\beta} \right) p, \\ \mathcal{M}_{6c}^{\mu\nu} &= g_{\rho \Lambda_c \Sigma_c} g_{D^* N \Sigma_c} \frac{1}{u - m_{\Sigma_c}^2} \\ &\times \bar{\Lambda}_c \gamma^\mu (\not{k}_2 - \not{k}_3 + m_{\Sigma_c}) \gamma^\nu p, \\ \mathcal{M}_{7a}^\mu &= ig_{DN\Lambda_c} g_{D^* N \Lambda_c} \frac{1}{s_1 - m_{\Lambda_c}^2} \\ &\times \bar{p} \gamma^\mu (\not{k}_1 + \not{k}_2 + m_{\Lambda_c}) \gamma_5 p, \\ \mathcal{M}_{7b}^\mu &= ig_{DN\Lambda_c} g_{D^* N \Lambda_c} \frac{1}{u - m_{\Lambda_c}^2} \\ &\times \bar{p} \gamma_5 (\not{k}_2 - \not{k}_3 + m_{\Lambda_c}) \gamma^\mu p, \\ \mathcal{M}_{8a}^{\mu\nu} &= g_{D^* N \Lambda_c}^2 \frac{1}{s_1 - m_{\Lambda_c}^2} \bar{p} \gamma^\nu (\not{k}_1 + \not{k}_2 + m_{\Lambda_c}) \gamma^\mu p, \end{aligned}$$

$$\mathcal{M}_{8b}^{\mu\nu} = g_{D^* N \Lambda_c}^2 \frac{1}{u - m_{\Lambda_c}^2} \bar{p} \gamma^\mu (\not{k}_2 - \not{k}_3 + m_{\Lambda_c}) \gamma^\nu p. \quad (9)$$

As in the case of charmed hadron production from the reaction $pp \rightarrow \bar{D}^0 p \Lambda_c^+$, total cross section for the reaction $pp \rightarrow \bar{D}^{*0} p \Lambda_c^+$ can be expressed in terms of off-shell cross sections for the subprocesses $\pi^0 p \rightarrow \bar{D}^{*0} \Lambda_c^+$, $\rho^0 p \rightarrow \bar{D}^{*0} \Lambda_c^+$, $\bar{D}^0 p \rightarrow \bar{D}^{*0} p$, and $\bar{D}^{*0} p \rightarrow \bar{D}^{*0} p$. In this case, the spin averaged differential cross section is

$$\begin{aligned} & \frac{d\sigma_{pp \rightarrow \bar{D}^0 p \Lambda_c^+}}{dtds_1} \\ &= \frac{g_{\pi NN}^2}{16\pi^2 s p_i^2} k \sqrt{s_1} (-t) \frac{1}{(t - m_\pi^2)^2} \sigma_{\pi^0 p \rightarrow \bar{D}^{*0} \Lambda_c^+}(s_1, t), \\ &+ \frac{3g_{\rho NN}^2}{32\pi^2 s p_i^2} k \sqrt{s_1} \frac{1}{(t - m_\rho^2)^2} [4(1 + \kappa_\rho)^2 \\ &\times (-t - 2m_N^2) \kappa_\rho \frac{(4m_N^2 - t)^2}{2m_N^2} + 4(1 + \kappa_\rho) \\ &\times \kappa_\rho (4m_N^2 - t)] \sigma_{\rho^0 p \rightarrow \bar{D}^{*0} \Lambda_c^+}(s_1, t) \\ &+ \frac{g_{D^* N \Lambda_c}^2}{16\pi^2 s p_i^2} k \sqrt{s_1} (-t + (m_N - m_{\Lambda_c})^2) \\ &\frac{1}{(t - m_D^2)^2} \sigma_{\bar{D}^0 p \rightarrow \bar{D}^{*0} p}(s_1, t) \\ &+ \frac{3g_{D^* N \Lambda_c}^2}{32\pi^2 s p_i^2} k \sqrt{s_1} \frac{1}{(t - m_{D^*}^2)^2} \\ &[-4t + 4(m_{\Lambda_c} - m_N)^2 - 8m_{\Lambda_c} m_N \\ &+ \frac{2(m_N^2 - m_{\Lambda_c}^2 - t)(m_N^2 - m_{\Lambda_c}^2 + t)}{m_{D^*}^2} \\ &+ \frac{2((m_{\Lambda_c} - m_N)^2 + t)t}{m_{D^*}^2}] \\ &\times \sigma_{\bar{D}^{*0} p \rightarrow \bar{D}^{*0} p}(s_1, t). \end{aligned} \quad (10)$$

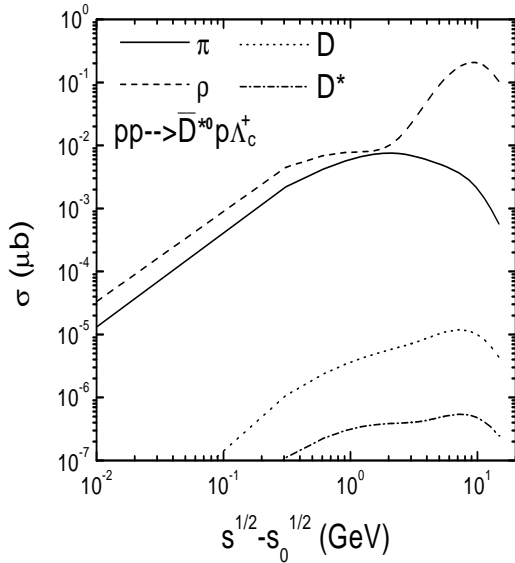


FIG. 6. Cross sections for charmed hadron production from $pp \rightarrow \bar{D}^{*0} p \Lambda_c^+$ due to pion (solid curve), rho meson (dashed curve), D (dotted curve), and D^* (dash-dotted curve).

Using coupling constants and cutoff parameters introduced in Section II, we have evaluated the cross section for the reaction $pp \rightarrow \bar{D}^{*0} p \Lambda_c^+$. In Fig. 6, we show contributions from pion (solid curve), rho meson (dashed curve), D (dotted curve), and D^* (dash-dotted curve) exchanges as functions of center-of-mass energy. As for the reaction $pp \rightarrow \bar{D}^0 p \Lambda_c^+$, light meson exchanges are more important than those from heavy meson exchanges. However, the contribution from rho exchange is larger than that from pion exchange, which is opposite to that in the reaction $pp \rightarrow \bar{D}^0 \Lambda_c^+$, as a result of couplings involving three vector mesons, which are absent in the latter reaction.

IV. TOTAL CROSS SECTION FOR CHARMED HADRON PRODUCTION IN PROTON-PROTON COLLISIONS

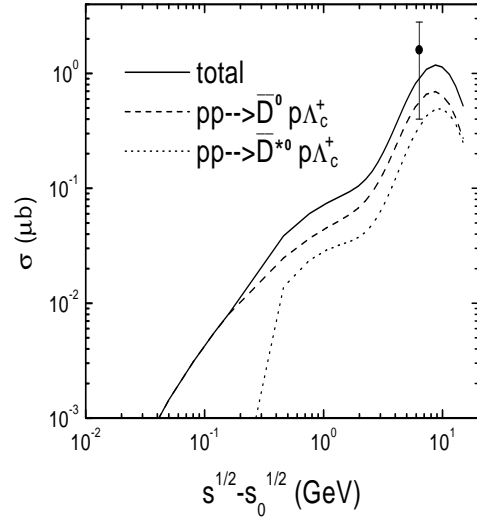


FIG. 7. Cross sections for charmed hadron production from proton-proton collisions. Dashed and dotted curves are for $pp \rightarrow \bar{D}^0 p \Lambda_c^+$ and $pp \rightarrow \bar{D}^{*0} p \Lambda_c^+$, respectively, while the total cross section is shown by solid curve. The threshold energy s_0 refers to that of the reaction $pp \rightarrow \bar{D}^0 p \Lambda_c^+$. Experimental data are shown by filled circles [22].

The total cross section for charm production from proton-proton collisions is shown in Fig.7 as a function of center-of-mass energy (solid curve). It's value at center-of-mass energy of 11.5 GeV is about $1 \mu\text{b}$ and is within the uncertainty of measured inclusive charm production cross section, which is about $2 \mu\text{b}$ as shown by solid circles with error bar [22]. The cross section decreases as energy drops and is about 1 nb at 40 MeV above threshold.

Also shown in Fig.7 are the cross section for the reactions $pp \rightarrow \bar{D}^0 p \Lambda_c^+$ (dashed curve) and $pp \rightarrow \bar{D}^{*0} p \Lambda_c^+$ (dotted curve), and it is seen that the former is somewhat larger than the latter.

V. SUMMARY

Using a hadronic model based on SU(4) flavor invariant Lagrangian with empirical masses and coupling constants, we have studied charmed hadron production from proton-proton collisions through the reactions $pp \rightarrow \bar{D}^0 p \Lambda_c^+$ and $pp \rightarrow \bar{D}^{*0} p \Lambda_c^+$. These reactions involve exchange of pion, rho meson, D , and D^* , and their cross sections can be expressed in terms of the cross sections for the off-shell processes $Mp \rightarrow \bar{D}^0 \Lambda_c^+$ and $Mp \rightarrow \bar{D}^{*0} \Lambda_c^+$, where M denotes one of the above exchanged off-shell mesons. With cutoff parameters of form factors adjusted to fit the cross section for strange hadron production in proton-proton reactions, the resulting cross section for charmed hadron production from proton-proton collisions at center-of-mass energy of 11.5 GeV is consistent with available experimental data. The predicted cross section at 40 MeV above threshold is about 1 nb. Our results will be useful for the experiments to be carried out at proposed accelerator at the German Heavy Ion Research Center [13].

ACKNOWLEDGMENT

This paper is based on work supported by the National Science Foundation under Grant No. PHY-0098805 and the Welch Foundation under Grant No. A-1358. SHL is also supported in part by the KOSEF under Grant No. 1999-2-111-005-5 and by the Korea Research Foundation under Grant No. KRF-2002-015-CP0074.

- [1] S.G. Matinyan and B. Müller, Phys. Rev. C **58**, 2994 (1998).
- [2] K.L. Haglin, Phys. Rev. C **61**, 031902(R) (2000); *ibid.* C **63**, 065201 (2001).
- [3] Z. Lin and C.M. Ko, Phys. Rev. C **62**, 034903 (2000).
- [4] Y. Oh, T. Song, and S.H. Lee, Phys. Rev. C **63**, 034901 (2001).
- [5] W. Cassing and C.M. Ko, Phys. Lett. B **396**, 39 (1997); W. Cassing and E.L. Bratkovskaya, Nucl. Phys. **A623**, 570 (1997).
- [6] N. Armesto and A. Capella, Phys. Lett. B **430**, 23 (1998).
- [7] W. Liu, C.M. Ko and Z.W. Lin, Phys. Rev. C **65**, 015203 (2001).
- [8] W. Liu, S.H. Lee, and C.M. Ko, Nucl. Phys. **A724**, 375 (2003).
- [9] W. Liu, C.M. Ko, Phys. Lett. B **533**, 259 (2002).
- [10] W. Cassing, L.A. Kondratyuk, G.I. Lykasov, and M.V. Rzjanin, Phys. Lett. B **513**, 1 (2001).
- [11] Z. Lin, C.M. Ko, and B. Zhang, Phys. Rev. C **61**, 024904 (2000).
- [12] Z. Lin, T.G. Di, and C.M. Ko, Nucl. Phys. **A689**, 965 (2001).
- [13] See <http://www/gsi.de/GSI-future>.
- [14] A.M. Gasparyan, V.Y. Grishina, L.A. Kondratyuk, W. Cassing, and J. Speth, nucl-th/0210018.
- [15] M.P. Rekalo and E. Tomasi-Gustafsson, Eur. Phys. Jour. A **16**, 575 (2003).
- [16] B. Holzenkamp, K. Holinde, and J. Speth, Nucl. Phys. **A500**, 485 (1989); G. Janssen, J.W. Durso, K. Holinde, B.C. Pearce, and J. Speth, Phys. Rev. Lett. **71**, 1978 (1993).
- [17] G. Janssen, K. Holinde, and J. Speth, Phys. Rev. C **54**, 2218 (1996).
- [18] F.S. Navarra, M. Nielsen, and M.E. Bracco, Phys. Rev. D **65** 037502 (2002).
- [19] R.A. Adelseck and B. Saghai, Phys. Rev. C **42**, 108 (1990).
- [20] C.H. Li and C.M. Ko, Nucl. Phys. **A712**, 110 (2002).
- [21] G.Q. Li, C.-H. Lee and G.E. Brown, Nucl. Phys. **A625**, 372 (1997).
- [22] N.S. Amaglobeli *et al.* (SVD Collaboration), Phys. Atom. Nucl. **64**, 891 (2001).